Photo-control of peptide conformation on a timescale of seconds with a conformationally constrained, blue-absorbing, photo-switchable linker

Andrew A. Beharry, Oleg Sadovski and G. Andrew Woolley*

Received 24th June 2008, Accepted 22nd August 2008
First published as an Advance Article on the web 24th September 2008
DOI: 10.1039/b810533b

Azobenzene derivatives can be used to reversibly photo-regulate conformation and activity when introduced as intramolecular bridges in peptides and proteins. Here we report the design, synthesis, and characterization of an azobenzene derivative that absorbs between 400–450 nm in aqueous solution to produce the *cis* isomer, and relaxes back to the *trans* isomer with a half-life of a few seconds at room temperature. In the *trans* form, the linker can span a distance of approximately 25 Å, so that it can bridge Cys residues spaced *i*, *i* + 15 in an α-helix. Switching of the azobenzene cross-linker from *trans* to *cis* causes a decrease in the helix content of peptides where the linker is attached *via* Cys residues spaced at *i*, *i* + 15 and *i*, *i* + 14 positions, no change in helix content with Cys residues spaced *i*, *i* + 11 and an increase in helix content in a peptide with Cys residues spaced at *i*, *i* + 7. In the presence of 10 mM reduced glutathione, the azobenzene cross-linker continued to photo-switch after 24 hours. This cross-linker design thus expands the possibilities for fast photo-control of peptide and protein structure in biochemical systems.

Introduction

Reversible optical control of protein structure offers the possibility of remote control of protein function in a variety of environments.[1–5] The azobenzene chromophore exhibits numerous desirable properties for use as an optical switch including robust reversibility and good quantum yields.[6] In applying azobenzenes to direct protein conformational change in biochemical systems, a number of requirements must be met. These include (i) a substantial structural change associated with isomerization that can be coupled to protein conformational change, (ii) a suitable wavelength and rate of thermal relaxation, (iii) stability in a cellular environment.

The effectiveness of conformational control will depend to a large degree on the end-to-end distance of the chromophore and how this changes upon isomerization. Certain urea and carbamate-substituted azobenzene derivatives, in particular, can accommodate a wide range of end-to-end distances in their *cis* isomers,[7] a feature that may limit their ability to affect the conformation of an attached peptide or protein.[8] A minimum number of bonds or a conformational constraint between the azo moiety that isomerizes and the peptide/protein backbone is likely to maximize the conformational switching effect.[9,10]

For unmodified azobenzene, the wavelength of maximal absorption of the more stable *trans* isomer occurs at 340 nm.[6] Light of this wavelength is scattered strongly by biological samples and can be absorbed by cellular constituents (*e.g.* NADH). Longer wavelengths lead to less light scattering and better penetration in biological samples.[11] Since the absorption spectra of *trans* and *cis* forms of azobenzenes overlap extensively, irradiation typically produces photostationary states of ~80% *cis* or ~95% *trans*.[6,12] This fact limits the degree of photo-switching that is possible; *e.g.* the fraction of *cis* isomer can be changed from 5% to 80% (16-fold).[12] Thermal isomerization, in contrast, yields >99.99% *trans* isomer.[7] Thus, to maximize the extent of photo-switching, it is preferable to use thermal isomerization to reset the switch; in that way, a much greater fold change in the *cis* isomer is possible. Since many cellular signaling processes operate on the time frame of seconds to minutes (*e.g.* ref. 13,14), the switch resetting process should occur at least on this timescale. The half-life for thermal *cis*-to-*trans* isomerization of unmodified azobenzene is on the order of 3–4 days at room temperature; however, this can be varied substantially by altering the nature of substituents on the aromatic rings (*e.g.* ref. 15–18). For instance, an amino-substituted azobenzene compound relaxes with a half-life of ~50 ms at room temperature.[19]

Finally, the photo-switch must be chemically stable under the desired operating conditions. Whereas azobenzenes are generally robust photo-switches, if they are to operate intracellularly, they must be stable to the reducing environment created by the presence of glutathione at millimolar concentrations.[20,21] Such an environment precludes the use of disulfide linkages for attaching the photo-switch as was used previously.[19] In addition, the N=N double bond itself may be sensitive to reduction in certain cases.[22,23]

With these considerations in mind, we designed the thiol-reactive azobenzene-based photo-switch **5**. We report here the synthesis and characterization of this new photo-switch.

Results and discussion

Design and synthesis of the cross-linker

We wished to create a long-wavelength absorbing, conformationally constrained, cross-linker to permit effective coupling of the geometrical change at the azo group with the peptide backbone. Linkages of photo-switches to Cys residues (as opposed to Lys (*e.g.* ref. 24)) ensure a minimum number of single bonds

Department of Chemistry, University of Toronto, 80 St. George St., Toronto, ON, M5S 3H6, Canada. E-mail: awoolley@chem.utoronto.ca; Fax: (416) 978-0675; Tel: (416) 978-0675

(four rotatable sigma bonds) between the cross-linker and the backbone. So that it might be stable in the reducing intracellular environment, we wished the linker to produce thioether linkages, rather than disulfides,[19] with peptide Cys residues. Based on previous studies,[18,19] we expected that an azobenzene derivative with a dialkylamino substituent in the *para* position would exhibit a wavelength of maximal absorption substantially longer than alkyl and amide substituted azobenzene derivatives, together with a faster thermal relaxation rate. These considerations led us to the design of **5**, which was synthesized as outlined in Scheme 1.

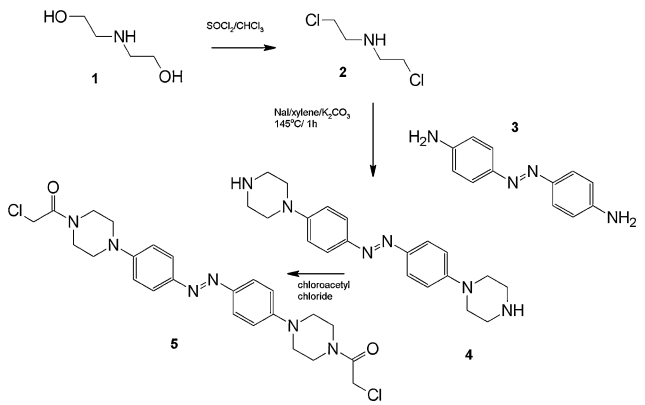

Scheme 1

The yield of the first step was excellent, however, yields for step two and three were poor (7%) and modest (33%), respectively. Although protection of the amino group in (**2**) would be expected to increase the yield in the second step, isolation of **4** by silica gel chromatography was straightforward and the direct route avoided two extra steps (protecting group introduction and removal). The cross-linker (**5**) was then reacted with the peptides shown in Fig. 1. The peptide sequences including the incorporation of the non-natural Aib residue in peptide JRK-7 were designed as described previously.[7] Reaction with AB-15, FZ-14, FK-11W and JRK-7, produces an intramolecular cross-link between Cys residues spaced *i*, *i* + 15, *i*, *i* + 14, *i*, *i* + 11, and *i*, *i* + 7, respectively. As a control, the cross-linker was also reacted with two molecules of the small tripeptide glutathione, which is too short to exhibit substantial secondary structure in solution. The cross-linked peptides were purified by HPLC and characterized by mass spectrometry.

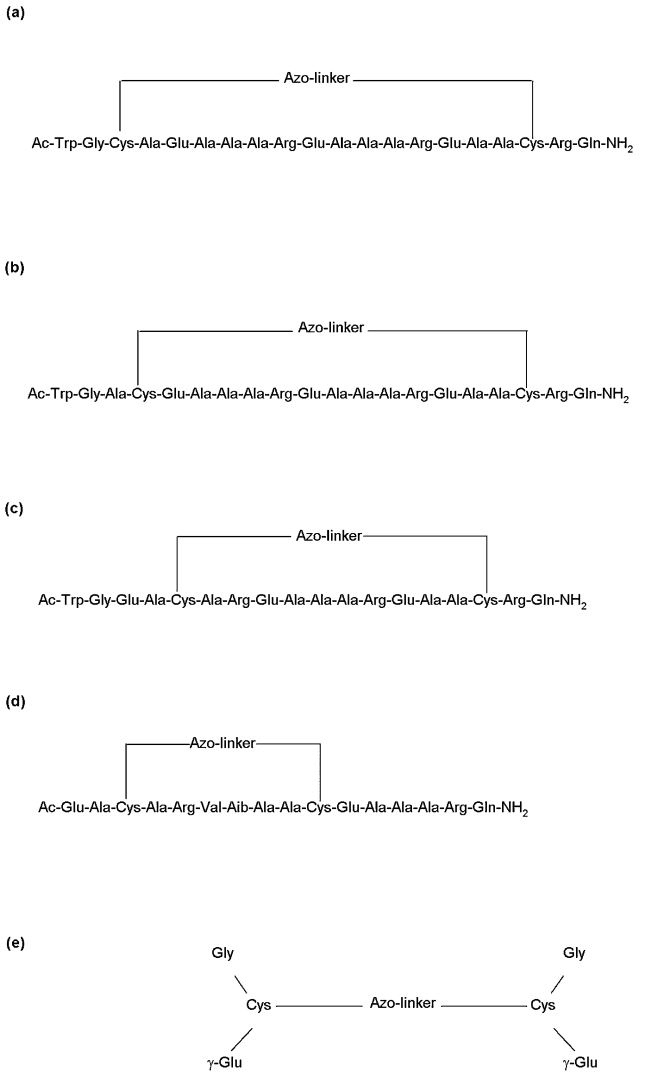

Fig. 1 Primary sequences of the cross-linked peptides examined in this study: (a) AB-15 (azo-linker **5** reacted *via* Cys residues spaced *i*, *i* + 15); (b) FZ-14 (azo-linker **5** reacted *via* Cys residues spaced *i*, *i* + 14); (c) FK-11W (azo-linker **5** reacted *via* Cys residues spaced *i*, *i* + 11); (d) JRK-7 (azo-linker **5** reacted *via* Cys residues spaced *i*, *i* + 7); (e) cross-linked glutathione.

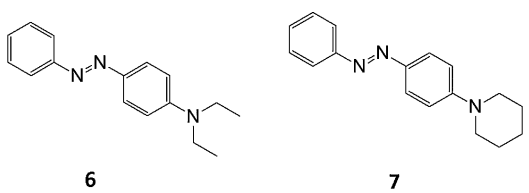

UV–Vis spectra: solvent and pH dependence

Fig. 2 shows a representative UV–Vis spectrum of the cross-linker attached to a peptide (FK-11W) obtained in aqueous buffer (pH 7.0). A broad maximum near 450 nm is observed that is shifted to shorter wavelengths relative to the unconstrained diamino-substituted azobenzene studied previously (λ_{max} ~480 nm).[19]

Hallas *et al.*[25,26] have studied the effects of cyclic *vs.* acyclic alkylamino substituents on azobenzene dyes (*e.g.* compounds **6**, **7**) and reported a similar hypsochromic shift in the UV absorbance of the cyclic compound (**7**).

Molecular modeling of **7** using the AM1 method shows that the piperidine ring is twisted relative to the phenyl ring and the nitrogen exhibits sp^3 character (Fig. 3). This conformation is preferred to reduce steric interactions between the equatorial protons on the piperidine ring with the *ortho* protons on the phenyl ring.[25,27] Rotation of the piperidine ring reduces the extent of π-overlap between the lone pair on the N atom and the adjacent aromatic π-electrons thereby bringing about a hypsochromic shift of λ_{max}.[25,26] A decreased resonance interaction between the N-atom

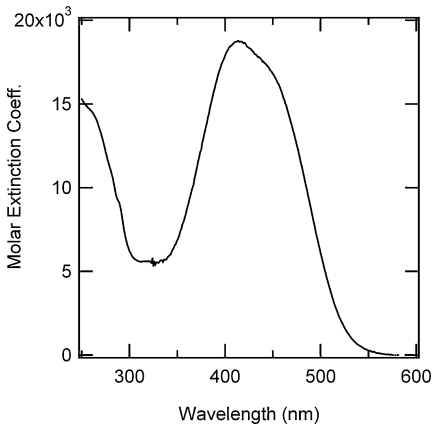

Fig. 2 UV–Vis spectrum of the cross-linker attached to the peptide FK-11W in 10 mM sodium phosphate buffer, pH 7.0, 22 °C.

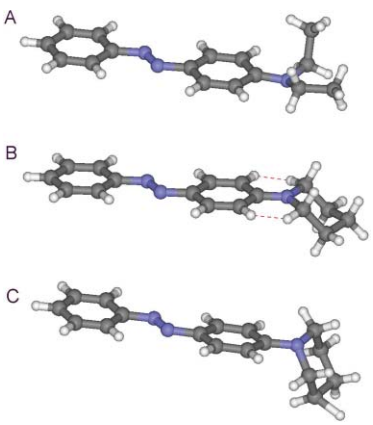

Fig. 3 Models of compounds (**6**) (A) and (**7**) (B, C). Whereas rotation of diethylamino groups in **6** can permit orbital overlap between the N atom lone pair and the aromatic system (A), for **7**, the piperidine ring structure leads to steric overlap of *ortho* protons if the N-atom is fully sp^2 hybridized (steric clashes are indicated by red dashed lines) (B). Steric overlap is relieved and the N atom becomes more sp^3-like as the piperidine ring is rotated relative to the aromatic system in the AM1 minimized structure (C).

and the aromatic system for the cyclic compound is supported by ^{13}C-NMR shift data.[28]

The UV–Vis spectrum of the cross-linker changes somewhat in shape and intensity depending on which peptide it is attached to. Addition of co-solvents (methanol/propanol/acetonitrile) is also observed to change the shape and intensity of the spectrum (*cf.* Fig. 2 *vs.* Fig 5). Although such changes have previously been ascribed to self-association of azo dyes,[29] we found a linear absorbance *vs.* concentration relationship over the concentration ranges examined, no dependence of the spectra on temperature (up to 80 °C in aqueous buffer), and no effect of cross-linked peptide concentration on thermal relaxation kinetics (see below).

Fig. 4 shows UV spectra of the cross-linker in aqueous buffer at a series of pH values from 1 to 7. At pH values of 5 and above, only the single broad maximum near 450 nm was observed. As the pH is lowered below 5, a second absorption band emerges near 600 nm. Based on previous studies with aminoazobenzenes,[26,27] the protonated cross-linker is expected to be in tautomeric equilibrium between the ammonium and azonium species (Scheme 2); the latter accounting for the absorbance near 600 nm.

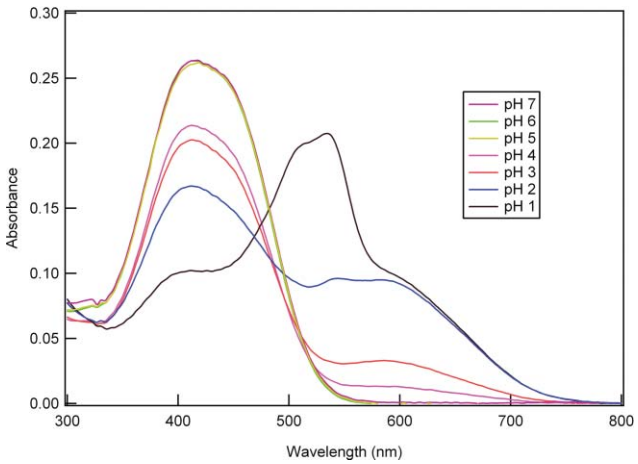

Fig. 4 UV–Vis spectra of cross-linker (attached to glutathione) in aqueous buffer (~15 μM) at a series of pH values.

Protonated forms of the cross-linker do not appear to isomerize. Thus, the effective pH range of this cross-linker is pH 5 and above. Since most biological systems of interest operate in the region of pH 7, this pH sensitivity is not likely to be problematic.

Photokinetic analysis: calculation of the absorption spectrum of the *cis* isomer

The UV–Vis spectrum of the *cis* isomer could not be obtained directly due to the fast rate of thermal *cis*-to-*trans* relaxation. Therefore, the absorption spectrum of the *cis* isomer was calculated using the photokinetic method previously employed for diamidoazobenzenes.[30] Photokinetic curves were obtained upon irradiation of cross-linked AB-15 in 50% methanol at 2 °C as described in the Experimental section. These conditions were

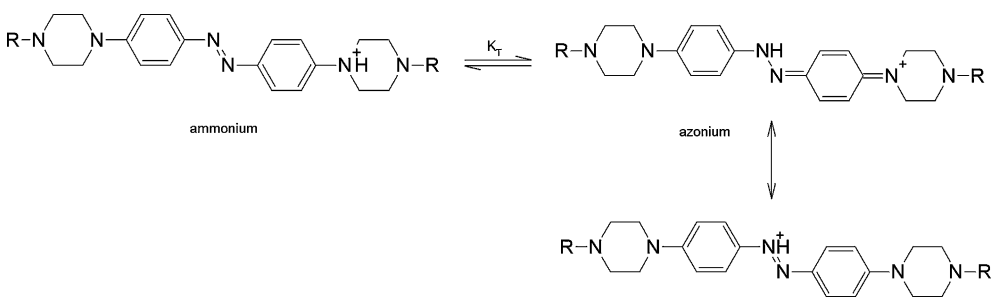

Scheme 2

chosen to maximize the % *cis* isomer that formed and to permit comparison with CD obtained under the same solvent conditions (see below). Fig. 5 shows the calculated spectrum of the pure *cis* isomer, together with the directly measured spectrum of the *trans* isomer. The *cis* spectrum shows a minimum at 400 nm, where the spectrum of the *trans* isomer is at a maximum. The wavelength of 400 nm is thus optimal for irradiation when the maximum % *cis* is desired. Based on the estimated *trans* → *cis* and *cis* → *trans* quantum yields obtained from the photokinetic analysis (approx. 0.1 and 0.5 respectively), a maximum of ~50% *cis* isomer is possible with 400 nm radiation of sufficient intensity.

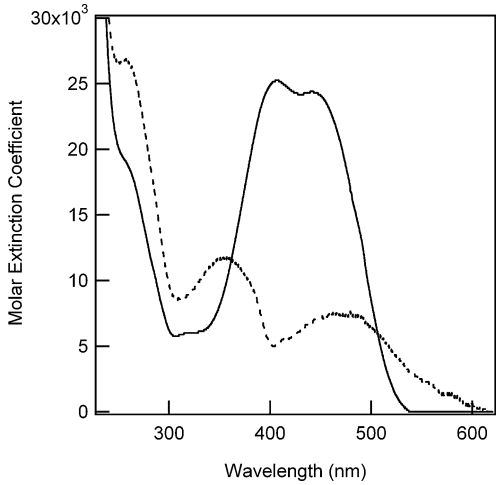

Fig. 5 The calculated absorption spectrum of the *cis* isomer (dashed line) of cross-linked AB-15 in 50% methanol in 10 mM sodium phosphate buffer pH 7.0. The spectrum of the *trans* isomer (solid line) in the same solvent is shown for reference.

Kinetics of thermal relaxation

If the cross-linker can relax to the *trans* isomer rapidly *via* a thermal process, essentially 100% *trans* isomer can be quickly obtained in the dark, thereby maximizing the change in concentration of *cis* isomer upon switching (*i.e.* <0.01% *cis* to 50% *cis* upon irradiation at 400 nm).

Previously, we found the dialkylamino-substituted azobenzene to be sensitive to changes in solvent polarity.[19] We therefore wished to test the effect of methanol on the rate of thermal relaxation. *cis* Isomers were produced by exposure to 400 nm light. Thermal relaxation to the *trans* isomer was measured by monitoring recovery of 450 nm absorbance over time. Data were fit to exponential decay curves and time constants calculated. The data are collected in Table 1.

In aqueous solution, half-lives on the order of a few seconds were obtained (Table 1). Depending on which peptide the cross-linker is attached to, the observed half-life varies by approximately a factor of 20. For X-JRK-7, a slow and a fast process were observed, suggesting the presence of more than one *cis*-state conformation. Multiple *cis*-state conformations have previously been observed by Renner *et al.* in studies with a cyclic azobenzene-containing peptide.[31] In the present case, it is possible that these correspond to different twist senses of the azo group relative to the peptide.[32] Half-lives did not appear to be sensitive to dilution, indicating that multiple time constants were not a result of self-association of peptides. With increasing percentages of methanol, the half-lives of the cross-linked peptides increased and mono-exponential relaxation behavior was observed (Table 1). Decreased solvent polarity may slow relaxation by destabilizing the transition state for isomerization, which has been proposed to have dipolar character similar to that in the excited state.[33] Thus, the local environment created around the photo-switch when attached to a peptide or protein is an important factor in determining the timescale of switching, a finding consistent with the observed variability of half-lives for different peptides (Table 1). Overall, the half-lives observed are somewhat longer than that observed for the acyclic dialkyl amino cross-linker studied previously[19] (where a ~50 ms half-life was observed in water and 1–20 s in 25–50% MeOH), consistent with a lesser degree of delocalization of the system (as discussed above). A half-life of ~1 s is nevertheless sufficiently rapid that ~100% *trans* isomer can be obtained, ~10–20 s after turning off irradiation, a timescale fast enough to permit probing of a wide variety of biochemical processes.

Effect of glutathione on photo-switching

In order to be of use for intracellular applications, photochemical switches must be stable to the reducing environment inside the cell. Typically, this environment is maintained by the small tripeptide glutathione present in its reduced form in ~1 mM concentrations.[20,21] Cross-linkers bearing disulfide linkages will be reductively cleaved rapidly under such conditions.[19] Glutathione is also known to reduce azo groups under certain conditions.[22,23] Moroder and colleagues have recently demonstrated that another azobenzene based peptide photo-switch was susceptible to reduction by glutathione.[23] The mechanism of reduction appears to involve attack of the thiol group of glutathione on the azo double bond to form a sulfenyl hydrazide adduct. This species

Table 1 Thermal relaxation half-lives (s) of cross-linked peptides

	In 10 mM phosphate buffer, pH 7.0		+25% MeOH		+50% MeOH	
Peptide	2 °C	25 °C	2 °C	25 °C	2 °C	25 °C
XAB15	4.0	1.8	9.0	4.0	34	8
XFZ14	7.0	3.8	8.2	5.8	53	18
XFK11	5.0	1.7	22	7.7	165	40
XJRK7	6(0.9)/91(0.1)[a]	2.3(0.74)/83(0.26)[a]	84	19	700	197
XGSH	0.5	—	2.6	1.0	22	6.7

[a] X-JRK-7 decays in phosphate buffer were fit to double exponential functions. Fast and slow time constants are shown with the fractional contribution of each process in brackets.

can react with a second molecule of glutathione to produce oxidized glutathione and the reduced hydrazo compound as products.[22,23] Alternatively, the sulfenyl hydrazide adduct may dissociate to reform the initial azo species. The rates of these reactions will depend on the glutathione concentration, the peptide concentration, as well as the redox potential of the cross-linker. The amino-substituted cross-linker studied here is expected to be less sensitive to reduction than the compound studied by Moroder and colleagues.[23]

The effect of glutathione on the photo-switching of the cross-linker attached to the peptide JRK-7 was studied in aqueous buffer pH 7.0 at 37 °C with 10 mM glutathione to mimic the intracellular reducing environment. This concentration of glutathione is at the high end of that normally found in cells.[20,21] This peptide was chosen because it had a relaxation rate slow enough to be measured conveniently under these solution conditions (Table 1). At 37 °C, X-JRK-7 displays a double exponential thermal relaxation process with half-lives of 1 s (55% of total decay) and 20 s (45%). The peptide was incubated with glutathione in the dark for 24 hours at 37 °C, to mimic conditions employed for loading cells in culture. Fig. 6 shows thermal relaxation and photoisomerization of cross-linked JRK-7 as monitored by measuring absorbance *vs.* time for 3 h after the 24 h dark incubation. Photo-switching appeared to be essentially unaffected (1 s (50% of total decay) and 22 s (50%)) (Fig. 6), probably as a result of the more electron-rich character of this azobenzene derivative compared to those studied previously.[10,23] The persistence of photo-switching for hours, even in the presence of 10 mM glutathione, indicates that the cross-linker should be functional in typical intracellular environments.

Conformational analysis of the cross-linker and effects of photoisomerization

To estimate the effects of the cross-linker on the conformational properties of attached peptides or proteins, we first examined the conformational properties of the cross-linker itself in *cis* and *trans* conformations. The range of end-to-end distances exhibited by the cross-linker provides a good first approximation for predicting its effect on conformational ensembles of helical peptides.[8,34] Simplified models of **5** after reaction with Cys residues of a peptide (where the β position of a cysteine side-chain is represented by a methyl group) in *cis* and *trans* conformation were built using HyperChem.

Fig. 7 shows histograms of the end-to-end (S–S) distances for *cis* and *trans* isomers, together with some representative structures. Depending on whether the Amber molecular mechanics forcefield or the semiempirical AM1 method is employed for calculating

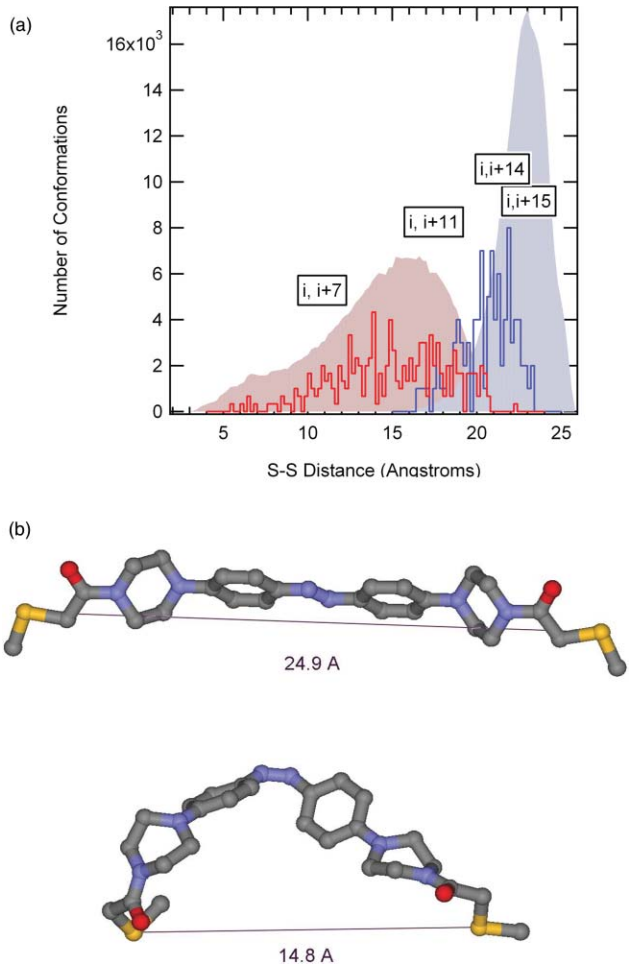

Fig. 7 (a) Probability distributions of distances between sulfur atoms in models of the cross-linker derived from the molecular dynamics simulations using the Amber forcefield (shaded areas), as well as conformational searches using the AM1 method (histograms) (*cis* (red), *trans* (blue)). Distances between S atoms within Cys residues spaced *i*, *i* + *x* in ideal α-helices are also indicated with boxes. The centre of the box is placed at the most probable distance and the box width indicates the range of distances possible, considering Cys side chain rotamers. (b) Representative structures and S–S distances observed (*trans*—top, *cis*—bottom).

conformational energies, the *trans* isomer has a most probable end-to-end distance of ~21–23 Å (and a range from 16 to 26 Å). The AM1 method tends to produce more sp^3-like tetrahedral geometry for the nitrogen atoms attached to the *para* positions of the azobenzene group when compared to the Amber forcefield, resulting in somewhat shorter end-to-end distances. Substantial

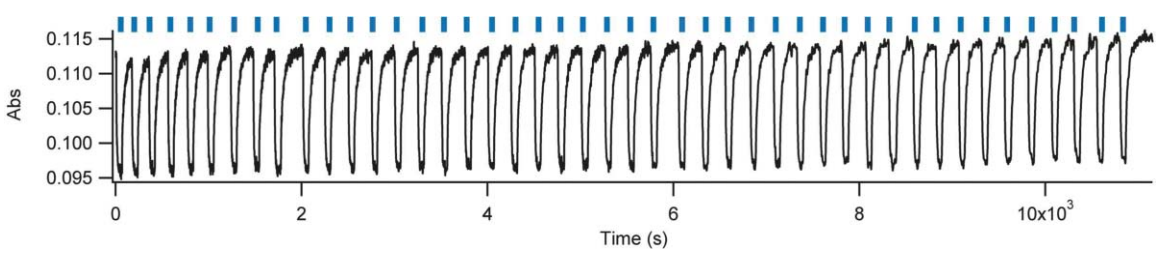

Fig. 6 Photo-switching of ~5 μM X-JRK-7 in phosphate buffer, pH 7.0, 37 °C with 10 mM reduced glutathione, as monitored by absorbance changes at 400 nm over the course of 3 h. Irradiation at 400 nm was present during the periods indicated by solid bars.

sp^3 character for these atoms is consistent with the spectral data described above. The *cis* isomer shows a broader distribution of end-to-end distances with a most probable distance of ~16 Å, but is compatible with distances from ~4 to ~21 Å.

For the *trans* form particularly, these end-to-end distances are significantly longer than for the diamino- and diamido-substituted azobenzenes studied previously so that this cross-linker can be used to span Cys residues more distant from one another in a peptide. Although the cyclic alkyl moiety limits the flexibility of the cross-linker compared to an analogous acyclic version, the molecular modeling suggests that there is still substantial flexibility associated with the cycloalkane rings so that a large range of end-to-end distances is still possible, especially for the *cis* isomer. An even more rigid derivative will perhaps be required to maximize the difference in end-to-end distance between *cis* and *trans* isomers.

Fig. 7(a) shows S–S spacing for Cys residues spaced *i*, *i* + 15, *i*, *i* + 14, *i*, *i* + 11, and *i*, *i* + 7, in an ideal α-helix. The *trans* distribution of the cross-linker fits best with the α-helical conformation of AB-15 (*i*, *i* + 15) and FZ-14 (*i*, *i* + 14) and least well with the JRK-7 (*i*, *i* + 7) peptide. Molecular modeling confirms the compatibility of the *trans* form of the cross-linker with a helical structure of FZ-14 and of the *cis* form of the cross-linker with a helical structure for JRK-7 (Fig. 8).

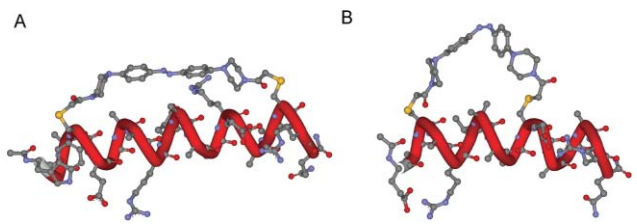

Fig. 8 Molecular models of (A) FZ-14 in an α-helical conformation with the *trans* form of the cross-linker attached; (B) JRK-7 in an α-helical conformation with the *cis* form of the cross-linker attached.

Fig. 9 shows CD spectra of uncross-linked and dark-adapted cross-linked peptides in aqueous buffer pH 7.0 at room temperature. As expected, cross-linked AB-15 and FZ-14 show the strongest helicity since the *trans* form of the linker is compatible with the helical structure in these peptides. In contrast, cross-linked JRK-7 is the least helical in the dark, since the *trans* form of the linker is not compatible with the helical structure in this peptide.

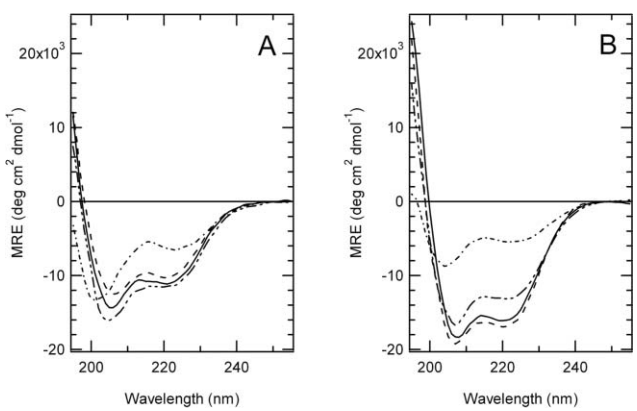

Fig. 9 CD spectra of uncross-linked (A) and dark-adapted cross-linked (B) peptides in aqueous phosphate buffer pH 7.0 at room temperature. AB-15 (—), FZ-14(– – –), FK-11W (– - - –), JRK-7 (– - –).

Based on observed effects with previous cross-linkers, one would predict that the *trans* form of the cross-linker (**5**) would be compatible with a helical conformation of AB-15 and FZ-14 (Fig. 7) and that isomerization from *trans* to *cis* would lead to a decrease in helical content. Conversely, a *trans* conformation of the cross-linker should be incompatible with the standard helix formation for JRK-7, but isomerization from *trans* to *cis* should make helix formation more likely. For FK-11W the *trans* and *cis* forms of the cross-linker appear to be about equally compatible with helical structure.

In order to test these predictions, we performed CD studies of the cross-linked peptides JRK-7, FK-11W, FZ-14 and AB-15 in pH 7.0 phosphate buffer–methanol (50 : 50), as described in the Experimental section. Although the co-solvent is likely to affect the % helix content, the same overall conformational behaviour is expected as in aqueous solution.[35] Under these mixed solvent conditions, the cross-linked peptides isomerize slowly enough to monitor using a conventional CD instrument. Photoisomerization produced ~45% of the *cis* isomer under these conditions, as determined from UV–Vis experiments. Fig. 10 shows the effects of photoisomerization on peptide conformation. As expected, relaxation from *cis* to *trans* after irradiation increases helicity for the cross-linked AB-15 and FZ-14 peptides, as evidenced by a stronger negative CD signal at 225 nm. Conversely, relaxation from *cis* to *trans* after irradiation decreases helicity for the JRK-7 cross-linked peptide, as evidenced by a weaker negative CD signal. No change in CD signal at 225 nm was observed for cross-linked FK-11W upon photoisomerization. The half-lives of *cis* forms of cross-linked peptides observed in the CD experiments are comparable to the half-lives estimated from the UV data in Table 1.

For cross-linked JRK-7, the half-life for thermal relaxation in the absence of methanol co-solvent is slow enough to permit CD kinetic measurements; these data are shown in Fig. 11. At low temperatures, the relaxation is dominated by a single decay process with a time constant near 5 s seen in both the UV data (Table 1) and the kinetic CD data (Fig. 11). Although the overall helix content is decreased in the absence of the co-solvent, the same trend is observed, *i.e. cis*-to-*trans* thermal relaxation leads to a decrease in helix content as evidenced by a weaker negative CD signal at 225 nm.

Summary

We have designed and synthesized a thiol-reactive azobenzene cross-linker that undergoes *trans*-to-*cis* photoisomerization upon irradiation at 400–450 nm and relaxes thermally with a half-life of about 1 s in aqueous solution. The cross-linker can be used to reversibly control the helical content of attached peptides. Its effects on helix content can be predicted by comparing the range of S–S distances in the intrinsic conformational ensemble of the peptide with the range compatible with the chemical structure of the linker. The *trans* form of the cross-linker is compatible with Cys residues spaced *i*, *i* + 15 and *i*, *i* + 14 in an α-helix, whereas the *cis* form of the cross-linker is compatible with Cys residues spaced *i*, *i* + 7. Photo-switching is maintained for many hours under reducing conditions similar to those found inside cells.

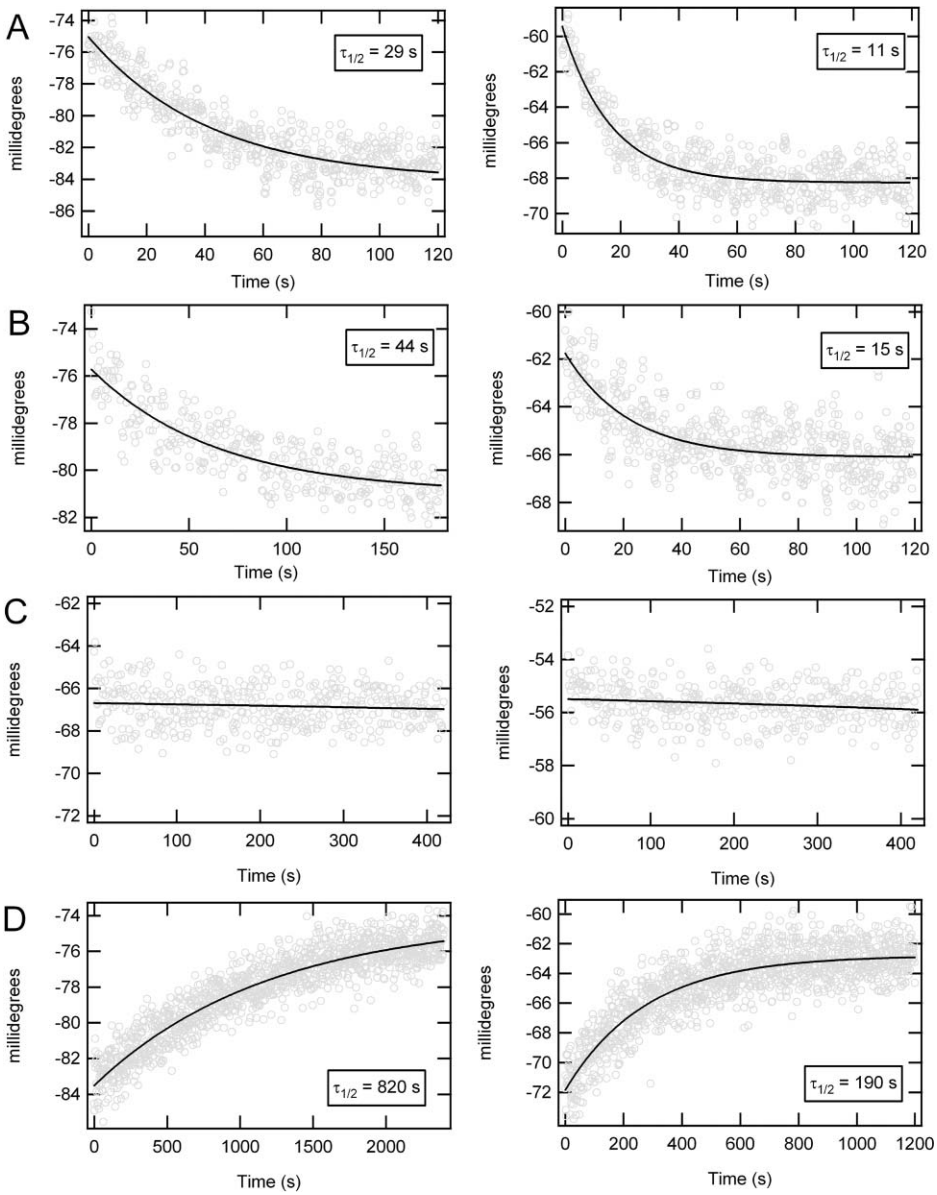

Fig. 10 Time-dependent circular dichroism (CD) signals at 225 nm after irradiation of (A) cross-linked AB-15 (~17 μM, 1 cm cell, 6 °C (left) 25 °C (right)); (B) cross-linked FZ-14 (~12 μM, 1 cm cell, 6 °C (left) 25 °C (right)); (C) cross-linked FK-11W (~17 μM, 1 cm cell, 6 °C (left) 25 °C (right)); (D) cross-linked JRK-7 (~37 μM, 1 cm cell, 6 °C (left) 25 °C (right)); solvent conditions: 50% methanol in phosphate buffer, pH 7.0.

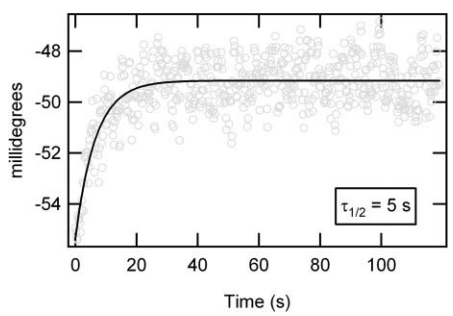

Fig. 11 Time-dependent circular dichroism (CD) signals at 225 nm after irradiation of cross-linked JRK-7 (~58 μM, 1 cm cell, 6 °C); in phosphate buffer, pH 7.0.

Experimental

All chemicals were purchased from Sigma-Aldrich Chemical Co., except if specified otherwise. All ^{1}H and ^{13}C NMR spectra were recorded using a Varian Unity 400 or a Varian Gemini 300 spectrometer. High resolution mass spectra were obtained either by electron impact (EI) or electrospray (ESI) ionization. Peptide mass spectra were obtained by MALDI ionization.

Synthesis of the cross-linker

Bis-(2-chloroethyl)-amine hydrochloride (2). 5 g (0.048 mol) of diethanolamine (**1**) were dissolved in 20 mL of chloroform and added dropwise with stirring to a solution of 14.15 g (0.11 mol) of thionyl chloride in 15 mL of chloroform. When all the amine had

been added, the volatile species were distilled off and the remaining material was recrystallized from acetone to give **2** (yield: 90%).

Bis-(4-piperazin-1-yl-phenyl)-diazene (4). A mixture of 2.5 g (0.012 mol) 4,4′-azobis-benzeneamine (**3**) (Alfa Aesar), 4.42 g (0.025 mol) **2**, 3.41 g (0.262 mol) potassium carbonate, 1.05 g (0.007 mol) sodium iodide and xylene (100 mL) was heated at 140–145 °C for 1 h. The cooled reaction mixture was poured into 200 mL water and then extracted with ethyl acetate (5 × 100 mL). The combined organic extracts were dried (Na_2SO_4), filtered, and the solvent was removed under reduced pressure to afford 1.8 g of a dark oil. Column chromatography on silica using ethyl acetate–methanol yielded 0.28 g of **4** (yield: 7%). ^{1}H-NMR (400 MHz, DMSO-d6) δ ppm 2.80–2.85 (m, 8H, 4 CH_2), 3.15–3.25 (m, 8H, 4 CH_2), 6.80 (s, 2H, 2NH), 7.00 (d, 9.4 Hz, 4H, 4CH), 7.70 (d, 9.4 Hz, 4H, 4CH). HRMS-ESI calc'd (MH+)($C_{20}H_{27}N_6$) 351.2291; obs'd 351.2278.

2-Chloro-1-[4-(4-{4-[4-(2-chloroacetyl)-piperazin-1-yl]phenyl-azo}-phenyl)-piperazin-1-yl]-ethanone (5). To a solution of 0.028 g (0.8 mmol) of **4** and 0.03 mL (0.28 mmol) of triethylamine in 4 mL CH_2Cl_2 was slowly added 0.017 mL (0.21 mmol) of chloroacetyl chloride. The reaction mixture was stirred overnight and the solvent was removed under reduced pressure. The residue was purified by column chromatography on silica (CH_2Cl_2–EtOAc) to give 0.16 g of **5** (yield: 33%). ^{1}H-NMR (300 MHz, DMSO-d6) δ ppm 3.30–3.35 (m, 4H), 3.40–3.45 (m, 4H), 3.60–3.65 (m, 8H), 4.4 (s, 4H), 7.1 (d, 9.1 Hz, 4H), 7.7 (d, 9.1 Hz, 4H). HRMS-ESI calc'd (MH+)($C_{24}H_{29}Cl_2N_6O_2$) 503.1723; obs'd 503.1702.

Peptide synthesis

Standard Fmoc-based solid-phase peptide synthesis was used to prepare the peptides AB-15 (Ac-WGCAEAAAREAAAREA-ACRQ-NH_2), FZ-14 (Ac-WGACEAAAREAAAREAACRQ-NH_2) and FK-11W (Ac-WGEACAREAAAREAACRQ-NH_2). The peptide JRK-7 (Ac-EACARVAibAACEAAARQ-NH_2) was purchased from Jerini Biotools (Berlin, Germany). The peptides AB-15, FZ-14 and FK-11 were constructed on PAL-resin (capacity 0.60 mmol g^{-1}). Coupling used 4 equivalents HATU, 6 equivalents DIPEA and 4 equivalents amino acid to give peptides AB-15 (yield: 52%), FZ-14 (yield: 55%) and FK-11W (yield: 50%). Peptides were purified by HPLC on a semipreparative SB-C18 column (Zorbax, 9.4 mm ID × 24 cm) using a linear gradient of 5–70% acetonitrile–H_2O (+0.1% trifluoroacetic acid) over the course of 30 min: AB-15 and FZ-14 eluted at 48% acetonitrile; FK-11W eluted at 47% acetonitrile; JRK-7 eluted at 50% acetonitrile. The peptides' molecular compositions were confirmed by MALDI-MS [M^+]: AB-15 ($C_{86}H_{140}N_{32}O_{29}S_2$) calc'd: 2131.0 Da; obs'd: 2131.8 Da, FZ-14 ($C_{86}H_{140}N_{32}O_{29}S_2$) calc'd: 2131.0 Da, obs'd: 2131.5 Da; FK-11W ($C_{80}H_{130}N_{30}O_{27}S_2$) calc'd: 1988.9 Da, obs'd: 1988.2 Da; JRK-7 ($C_{65}H_{114}N_{24}O_{23}S_2$) calc'd: 1644.8 Da, obs'd: 1644.4 Da.

Peptide cross-linking

Intramolecular cross-linking of Cys residues in AB-15 and FZ-14 was performed as follows: 2.1 mg (1.0 μmol) of AB-15 or FZ-14 and 0.29 mg (1.0 μmol) of tris(carboxyethyl)phosphine were dissolved in 150 μL of 50 mM Tris·Cl buffer (pH 8) and incubated for 1 h at room temperature to ensure cysteine residues were in their reduced state. The solution was stirred and 350 μL of a 5.7 mM solution of the linker in DMSO were added dropwise. Although DMSO is a mild oxidant, no effect on cross-linking was observed. The mixture was heated to 40 °C and left to stir for 24 h, protected from light. The modified peptides were purified by HPLC (SB-C18 column, as described above) using a linear gradient of 5–57% acetonitrile–H_2O (+0.1% trifluoroacetic acid) over the course of 31 min (elution at 50% acetonitrile). The modified peptide compositions were confirmed by MALDI-MS [M^+]: calc'd for $C_{110}H_{166}N_{38}O_{31}S_2$ (cross-linked FZ-14) = 2563.8 Da; obs'd = 2564.1 Da; calc'd for $C_{110}H_{166}N_{38}O_{31}S_2$ (cross-linked AB-15) obs'd = 2562.8 Da.

Intramolecular cross-linking of Cys residues in FK-11W was performed as follows: 3.0 mg (1.5 μmol) of FK-11W and 0.43 mg (1.5 μmol) of tris(carboxyethyl)phosphine were dissolved in 300 μL of 15 mM Tris·Cl buffer (pH 8) and incubated for 1 h at room temperature to ensure cysteine residues were in their reduced state. The solution was stirred and 700 μL of a 4.2 mM solution of the linker in DMSO were added dropwise. The mixture was heated to 40 °C and left to stir for 24 h, protected from light. The modified peptide was purified by HPLC (SB-C18 column, as described above) using a linear gradient of 5–80% acetonitrile–H_2O (+0.1% trifluoroacetic acid) over the course of 45 min (elution at 49% acetonitrile). The modified peptide composition was confirmed by MALDI-MS [M^+]: calc'd for $C_{104}H_{156}N_{36}O_{29}S_2$ = 2421.6 Da; obs'd = 2421.1 Da.

Intramolecular cross-linking of Cys residues in JRK-7 was performed as follows: 1.0 mg (0.6 μmol) of JRK-7 and 0.17 mg (0.6 μmol) of tris(carboxyethyl)phosphine were dissolved in 150 μL of 50 mM Tris·Cl buffer (pH 8) and incubated for 1 h at room temperature to ensure cysteine residues were in their reduced state. The solution was stirred and 350 μL of a 3.4 mM solution of the linker in DMSO were added dropwise. The mixture was heated to 40 °C and left to stir for 24 h. The modified peptide was purified by HPLC (SB-C18 column, as described above) using a linear gradient of 5–57% acetonitrile–H_2O (+0.1% trifluoroacetic acid) over the course of 31 min (elution at 50% acetonitrile). The modified peptide composition was confirmed by MALDI-MS [M^+]: calc'd for $C_{89}H_{140}N_{30}O_{25}S_2$ = 2077.3 Da; obs'd = 2075.9 Da.

A glutathione derivative of the linker was prepared as follows: 100 μL of a 13 mM solution of glutathione in 50 mM Tris·Cl buffer (pH 8) was stirred and 50 μL of an 8.5 mM solution of the linker in DMSO were added. The mixture was heated to 40 °C and left to stir for 24 h, protected from light. The glutathione derivative was purified by HPLC (SB-C18 column, as described above) using a linear gradient of 5–50% acetonitrile–H_2O (+0.1% trifluoroacetic acid) over the course of 27 min (elution at 45% acetonitrile). The glutathione derivative molecular composition was confirmed by MALDI-MS [M^+]: calc'd for $C_{44}H_{60}N_{12}O_{14}S_2$ = 1045.1 Da; obs'd = 1044.3 Da.

UV–Vis spectra and photoisomerization

Ultraviolet absorbance spectra were obtained using either a Perkin-Elmer Lambda 2 spectrophotometer or using a diode array UV–Vis spectrophotometer (Ocean Optics Inc., USB4000) coupled to a temperature controlled cuvette holder (Quantum Northwest, Inc.). Measurements of thermal relaxation rates and

photokinetic experiments used the latter arrangement. Irradiation of the sample (at 90° to the light source and detector used for the absorbance measurements) was carried out using a xenon lamp (450 W, Osram 450XBO/2 OFR) coupled to a double monochromator. Rates of thermal *cis*-to-*trans* isomerization were measured for a series of temperatures by monitoring absorbance at 450 nm after irradiation to convert a percentage of the solution to the *cis* isomer. The light used for the absorbance measurement was of sufficiently low intensity to cause negligible isomerization. Solution conditions are described in the figure legends.

A molar extinction coefficient for the cross-linker of 16 800 M^{-1} cm^{-1} at 450 nm in pH 7.0 phosphate buffer was determined by comparing absorbance at 450 nm *vs.* 280 nm for the cross-linked peptide FK-11W. An extinction coefficient of 5625 M^{-1} cm^{-1} at 280 nm from the Trp residue at the N-terminus of the cross-linked FK-11W was used. The UV–Vis spectrum of cross-linked GSH (which does not have a Trp residue) was used to correct for contributions of the cross-linker to the measured absorbance at 280 nm.

Circular dichroism measurements

Circular dichroism (CD) measurements were performed on a Jasco Model J-710 spectropolarimeter. Tris(carboxyethyl)phosphine (1 mM) was present in the uncross-linked peptide samples to ensure that cysteine residues were in their reduced form. Peptide concentrations were determined using a molar extinction coefficient for the cross-linker of 16 800 M^{-1} cm^{-1} at 450 nm in pH 7.0 phosphate buffer. For fast CD measurements, the instrument was set to time-drive mode. Samples were dissolved in 10 mM pH 7.0 sodium phosphate buffer and/or 50% methanol in 10 mM pH 7.0 sodium phosphate buffer. Temperatures were measured using a microprobe directly in the sample cell. The nitrogen flow rate was increased to minimize condensation on the cuvette when the temperature of the sample was 6 °C. Samples in cuvettes were irradiated for 1 minute with a metal halide lamp (150 W, Osram HQI-SE150/NDX (unfiltered), then measured immediately.

Photokinetic analysis

Photokinetic analyses were performed essentially as described previously.[30] A solution of cross-linked AB-15 (~15 μM) was prepared in 50% methanol–50% phosphate buffer pH 7.0. Absorption spectra were recorded with the diode array UV–Vis spectrophotometer described above, using slits of 16 nm and 16 nm. Two wavelengths of irradiation (λ_1 = 390 nm and λ_2 = 405 nm), both within the π–π* band of the chromophore, were chosen for two sets of photokinetic measurements. In the first set, the cross-linked peptide solution was irradiated with 390 nm light and the absorbance at 390 nm and 450 nm were recorded. In the second set, the cross-linked peptide solution was irradiated with 405 nm light and the absorbance at 405 nm and 450 nm were recorded. A total irradiation time of 80–130 s was used with a 1 s sampling period. The intensity of the light was determined directly in the working cell using an aqueous solution of potassium ferrioxalate.[36] The working cell was a quartz cuvette of 1 cm path length with a stir bar containing 1 mL of the cross-linked peptide solution. Data was analyzed as described previously.[30]

Molecular modeling

Models of *cis* and *trans* cross-linkers were built using HyperChem (v.8, Hypercube Inc.), with the linker terminated with methyl groups representing the β carbon of Cys in the cross-linked peptide, and minimized using the Amber99 forcefield. Restraints were added to the azo bond for the *cis* conformation (force constant 16). Molecular dynamics runs were performed *in vacuo* essentially as described previously[19] with a distant dependent dielectric, and 1–4 scale factors of 0.833 for electrostatic and 0.5 for van der Waals interactions, a step size of 1 fs and 300 K as the simulation temperature. Trajectories were analyzed to verify that numerous torsion angle changes occurred for all single bonds during the course of the simulation to ensure that conformational space was adequately sampled. All points histograms were then produced for the S–S distance during the full set of simulations for each isomer.

Additional conformational searches were performed using the conformational search algorithm of HyperChem (v.8, Hypercube Inc.) and the AM1 method. The ranges for acyclic torsions and ring torsion flexing were ±60 to 180° and ±30 to 120°, respectively. A usage directed search algorithm was employed, with structures with non-H atom positions that varied by less than 0.25 Å RMS or with torsion angle changes less than 5° considered as duplicates. Structures less than 6 kcal mol^{-1} in energy above the lowest found were retained.

Acknowledgements

We are grateful to the Natural Sciences and Engineering Research Council of Canada for financial support.

References

1 C. Renner and L Moroder, *ChemBioChem*, 2006, **7**, 868.
2 G. A. Woolley, A. S. Jaikaran, M. Berezovski, J. P. Calarco, S. N. Krylov, O. S. Smart and J. R. Kumita, *Biochemistry*, 2006, **45**, 6075.
3 M. Volgraf, P. Gorostiza, R. Numano, R. H. Kramer, E. Y. Isacoff and D. Trauner, *Nat. Chem. Biol.*, 2006, **2**, 47.
4 Y. Liu and D. Sen, *J. Mol. Biol.*, 2004, **341**, 887.
5 A. M. Caamano, M. E. Vazquez, J. Martinez-Costas, L. Castedo and J. L. Mascarenas, *Angew. Chem., Int. Ed.*, 2000, **39**, 3104.
6 H. Rau, in *Photochromism. Molecules and Systems*, ed. H. Durr and H. Bouas-Laurent, Elsevier, Amsterdam, 1990, pp. 165–192.
7 N. Pozhidaeva, M. E. Cormier, A. Chaudhari and G. A. Woolley, *Bioconjugate Chem.*, 2004, **15**, 1297.
8 D. C. Burns, D. G. Flint, J. R. Kumita, H. J. Feldman, L. Serrano, Z. Zhang, O. S. Smart and G. A. Woolley, *Biochemistry*, 2004, **43**, 15329.
9 U. Kusebauch, S. A. Cadamuro, H. J. Musiol, M. O. Lenz, J. Wachtveitl, L. Moroder and C. Renner, *Angew. Chem., Int. Ed.*, 2006, **45**, 7015.
10 R. F. Standaert and S. B. Park, *J. Org. Chem.*, 2006, **71**, 7952.
11 W. Cheong, S. Prahl and A. Welch, *IEEE J. Quantum Electron.*, 1990, **26**, 2166.
12 D. A. James, D. C. Burns and G. A. Woolley, *Protein Eng.*, 2001, **14**, 983.
13 D. M. Bers and T. Guo, *Ann. N. Y. Acad. Sci.*, 2005, **1047**, 86.
14 U. S. Bhalla, *Curr. Opin. Genet. Dev.*, 2004, **14**, 375.
15 E. Talaty and J. Fargo, *J. Chem. Soc.*, 1967, 65.
16 R. Le Fevre and J. Northcott, *J. Chem. Soc.*, 1953, 867.
17 C. Forber, E. Kelusky, N. Bunce and M. Zerner, *J. Am. Chem. Soc.*, 1985, **107**, 5884.
18 N. Nishimura, T. Sueyoshi, H. Yamanaka, E. Imai, S. Yamamoto and S. Hasegawa, *Bull. Chem. Soc. Jpn.*, 1976, **49**, 1381.
19 L. Chi, O. Sadovski and G. A. Woolley, *Bioconjugate Chem.*, 2006, **17**, 670.
20 H. R. Lopez-Mirabal and J. R. Winther, *Biochim. Biophys. Acta*, 2008, **1783**, 629.

21 H. Ostergaard, C. Tachibana and J. R. Winther, *J. Cell Biol.*, 2004, **166**, 337.
22 E. Kosower and H. Kanety-Londner, *J. Am. Chem. Soc.*, 1976, **98**, 3001.
23 C. Boulegue, M. Loweneck, C. Renner and L. Moroder, *ChemBioChem*, 2007, **8**, 591.
24 K. Fujimoto, M. Amano, Y. Horibe and M. Inouye, *Org. Lett.*, 2006, **8**, 285.
25 G. Hallas, R. Marsden, J. Hepworth and D. Mason, *J. Chem. Soc., Perkin Trans. 2*, 1984, 149.
26 J. Hepworth, D. Mason, G. Hallas and R. Marsden, *Dyes Pigm.*, 1985, **6**, 389.
27 A. Bottini and C. Nash, *J. Am. Chem. Soc.*, 1962, **84**, 734.
28 C. Nash and G. Maciel, *J. Phys. Chem.*, 1964, **68**, 832.
29 J. Hamlin, D. Phillips and A. Whiting, *Dyes Pigm.*, 1999, **41**, 137.
30 V. Borisenko and G. A. Woolley, *J. Photochem. Photobiol., A*, 2005, **173**, 21.
31 C. Renner, J. Cramer, R. Behrendt and L. Moroder, *Biopolymers*, 2000, **54**, 501.
32 J. R. Kumita, O. S. Smart and G. A. Woolley, *Proc. Natl. Acad. Sci. U. S. A.*, 2000, **97**, 3803.
33 N. Nishimura, T. Tanaka, M. Asano and Y. Sueishi, *J. Chem. Soc., Perkin Trans. 2*, 1986, 1839.
34 G. A. Woolley, *Acc. Chem. Res.*, 2005, **38**, 486.
35 J. E. Brown and W. A. Klee, *Biochemistry*, 1971, **10**, 470.
36 S. Murov, I. Carmichael and G. Hug, *Handbook of Photochemistry*, Marcel Dekker, Inc, New York, 1993, pp. 299–305.

